Electronic Supplementary Information for:

An activatable nanoprobe based on nanocomposites of visible-light-excitable europium(III) complex-anchored MnO_2 nanosheets for bimodal time-gated luminescence and magnetic resonance imaging of tumor cells

Bo Song,*[a] Huinan Yan,[a] Jiao Jiang,[a] Jin Yu,[b] Shengjun Huang[c] and Jingli Yuan*[a]

[a] State Key Laboratory of Fine Chemicals, School of Chemical Engineering, Dalian University of Technology, Dalian 116024, China.

[b] Second Affiliated Hospital, Dalian Medical University, Dalian 116027, China.

[c] Division of Fossil Energy Conversion, Dalian Institute of Chemical Physics, Chinese Academy of Sciences, Dalian, 116023, China

E-mail: bo.song@dlut.edu.cn, jlyuan@dlut.edu.cn

Table of Contents

1. Experimental section

Materials and physical measurements

The ligands, 1-(biphenyl-4'-yl)-4,4,4-trifluorobutane-1,3-dione (HBTD) and 2-(N,N-diethylanilin-4-yl)-4,6-bis(3,5-dimethylpyrazol-1-yl)-1,3,5-triazine) (DPBT), and MnO_2 nanosheets were perpared according to the previously reported methods.[1-3] Tetramethylammonium hydroxide (TMAH), manganese chloride tetrahydrate ($MnCl_2 \cdot 4H_2O$), hydrogen peroxide (H_2O_2, 30 wt%), L-glutathione (GSH), N-ethylmaleimide (NEM), N-acetyl-L-cysteine (NAC) and 3-(4,5-dimethyl-2-thiazoyl)-2,5-diphenyltetrazolium bromide (MTT) were purchased from Sigma-Aldrich. Cultured HeLa, MCF-7, HepG2 and LO2 cells, KM mice and tumor-bearing BALB/c mice were provided by Dalian Medical University. Unless otherwise stated, all chemical materials were purchased from commercial sources and used without further purification.

The morphology of MnO_2 nanosheets was characterized with a JEOL JEM-2000EX transmission electron microscope (TEM). Zeta potential and dynamic light scattering (DLS) were measured by using Zetasizer Nano ZS90 UK. The AFM images of MnO_2 nanosheets were recorded on a Bruker Nanowizard 4XP atomic force microscope. ^1H NMR spectra were measured on a Bruker Avance spectrometer (400 MHz). Mass spectra were recorded on a Thermo G6224A TOF MS spectrometer. Elemental analysis was carried out on a Vario-EL analyzer. The contents of Mn were measured on a PerkinElmer Optima 2000DV inductively coupled plasma-optical emission spectrometer (ICP-OES). TGL spectra were measured on a Perkin-Elmer LS 50B luminescence spectrometer with the settings of delay time, 0.2 ms; gate time, 0.4 ms; cycle time, 20 ms; excitation slit, 8 nm; and emission slit, 8 nm. Absorption spectra were measured on a UV-1800 UV-Vis spectrophotometer (Shimadzu Instruments Suzhou Co., Ltd.). Luminescence lifetimes were measured on an Edinburgh FS5 spectrometer. All bright-field, steady-state and TGL imaging measurements were conducted on a laboratory-use luminescence microscope. The measurements of transverse and longitudinal relaxation times were performed on a 0.5 T NM12 MR analyzer (Suzhou Niumag Analytical Instrument Corporation). All the MRI measurements were carried out on an NMI20-030H-I MR imager (Suzhou Niumag Analytical Instrument Corporation).

Preparation of the nanoprobe and its application to bimodal TGL-MR detections of GSH and H_2O_2 in buffer

For quantifying the amount of [Eu(BTD)$_3$(DPBT)] on the surface of MnO_2 nanosheets, [Eu(BTD)$_3$(DPBT)] (3.3 μM) and MnO_2 nanosheets (287 μM) were mixed for 2 min at RT in 10 mM HEPES buffer of pH 7.4. The obtained [Eu(BTD)$_3$(DPBT)]@MnO_2 nanoprobe was separated by centrifugation using an Amicon Ultra centrifugal filter (pore size 10 kDa MWCO). The content of free [Eu(BTD)$_3$(DPBT)] in the filtrate was evaluated by the TGL assay.

Cyclic voltammetric (CV) analyses were carried out on an autolab electrochemical system (CHI600D, Shanghai) coupled with a three-electrode cell. The working electrode was a glassy carbon electrode, the auxiliary electrode was a platinum wire and all the potentials reported in this study have been measured against Ag/AgCl as a reference electrode. All the CV measurements were carried out at room temperature in a solution of 25 mL HEPES buffer (10 mM, pH = 7.4). The scanned area was in the potential range of -1.5 V to 1.0 V and the scan rate was 0.1 V/s. The $MnCl_2$ solution was chosen as the standard Mn^{2+} solution (120 μM). In order to verify GSH/H_2O_2-triggered the reduction of MnO_2 nanosheets to Mn^{2+}, the MnO_2 nanosheets and GSH/H_2O_2-MnO_2 nanosheets (120 μM MnO_2 nanosheets were incubated with 120 μM GSH or H_2O_2 for 2 min at room temperature) were subjected to CV measurements.

For TGL detections of GSH and H_2O_2 in buffer, the nanoprobe [Eu(BTD)$_3$(DPBT)]@MnO_2 was prepared by incubating 3.3 μM [Eu(BTD)$_3$(DPBT)] with 287 μM MnO_2 nanosheets for 2 min at RT in 0.01 M HEPES buffer (pH 7.4, containing 0.05% Triton X-100). The obtained nanoprobe solution was mixed with different concentrations of GSH and H_2O_2 for 5 min, and then the mixtures were subjected to TGL measurements.

For MR detections of GSH and H_2O_2 in buffer, the above as-prepared nanoprobe was mixed with various concentrations of GSH or H_2O_2 for 5 min. Then, the longitudinal and transverse relaxation times and MR images of the mixtures were measured on the MR analyzer and imager, respectively. For assessing the amount of free [Eu(BTD)$_3$(DPBT)] in the nanoprobe solution, the stock solution of [Eu(BTD)$_3$(DPBT)]@MnO_2 was separated by centrifugation using an Amicon Ultra centrifugal filter unit (pore size 10 kDa MWCO). The content of free [Eu(BTD)$_3$(DPBT)] in filtrate was evaluated by the TGL assay.

Response specificity investigation of the nanoprobe

To assess the response specificity of the nanoprobe to GSH and H_2O_2, the above as-prepared nanoprobe [Eu(BTD)$_3$(DPBT)]@MnO_2 was incubated with GSH (0.5 mM), H_2O_2 (0.5 mM), Cys (0.5 mM), Hcy (0.5 mM), NADH (0.5 mM), uric acid (0.5 mM), Vc (0.5 mM) and other interferents (1.0 mM) for 5 min, respectively. Then the TGL intensities and the transverse relaxation times of the mixtures were recorded.

Cytotoxicity and biocompatibility investigations of the nanoprobe

The cytotoxicity of the above as-prepared nanoprobe [Eu(BTD)$_3$(DPBT)]@MnO_2 to HeLa cells and LO2 cells was determined by MTT assay.[4] HeLa and LO2 cells cultured in Dulbecco's modified Eagle medium (DMEM) were washed with isotonic saline (ISS, 140 mM NaCl, 10 mM glucose, 3.5 mM KCl) before use, and then incubated with different concentrations of [Eu(BTD)$_3$(DPBT)]@MnO_2 (0, 50, 100, 150, 200, 250, 300, 350, 400 μM in Mn concentration) at 37 °C in a 5% CO_2 /95% air incubator for 24 h. After that, the cells were washed with ISS and incubated with 5 mg mL^{-1} MTT in an incubator for 4 h. After supernatants were removed, the cells was dissolved in 100 μL DMSO and the absorbance at 490 nm was measured.

For investigating the cytotoxicities of the Eu(III) complexes and Mn(II) ions, HeLa cells were incubated with the different concentrations of [Eu(BTD)$_3$(DPBT)] (0, 4.0, 8.0, 12.0, 16.0, 20.0 μM) and Mn(II) ions (0, 40, 80, 120, 160, 200 μM) at 37 °C in a 5% CO_2 /95% air incubator for 24 h, respectively. After that, the cells were washed with ISS and incubated with 5 mg/mL MTT in an incubator for 4 h. After supernatants were removed, the cells were dissolved in 100 μL DMSO and the absorbance at 490 nm was measured.

To further examine the biocompatibility of the nanoprobe [Eu(BTD)$_3$(DPBT)]@MnO_2, three KM mice (females, ~20 g body weight) were given [Eu(BTD)$_3$(DPBT)]@MnO_2 (200 μL, 11.5 μM [Eu(BTD)$_3$(DPBT)] mixed with 1.0 mM MnO_2 nanosheets in physiological saline solution) by intravenous injection. After 24 h, the mice were sacrificed by dislocating cervical vertebra and the main organs (heart, liver, spleen, lung, and kidney) were surgically dissected. The collected organs were fixed with 4% formaldehyde in PBS and embedded in paraffin. Then the standard hematoxylin and eosin (H&E) staining was carried out for histological analysis.

TGLI of live cells

HeLa (human cervical adenocarcinoma cell line), MCF-7 (human breast adenocarcinoma cell line), HepG2 (human hepatocellular carcinoma cell line) and LO2 (human hepatocyte cell line) cells were cultured in a glass bottom culture dishes in DMEM with 10% fetal bovine serum, 1% penicillin and 1% streptomycin at 37 °C in a 5% CO_2/95% air incubator. For staining cells, the cultured cells were washed three times with ISS, and then incubated with the nanoprobe [Eu(BTD)$_3$(DPBT)]@MnO_2 (4.6 μM [Eu(BTD)$_3$(DPBT)] mixed with 400 μM MnO_2 nanosheets) in 200 μl culture medium for 2 h. After thoroughly washing with ISS, the cells were subjected to the TGLI on the microscope with the conditions of gate time, 1.0 ms; delay time, 10 μs; lamp pulse width, 60 μs; and exposure time, 500 ms. For the control group, HeLa cells were pretreated with 50 μM NAC for 0.5 h and 50 μM NEM for 0.5 h, and then incubated with the nanoprobe for 2 h prior to being used for TGLI.

TGLI and MRI of tumor-bearing nude mice

To evaluate the performance of the nanoprobe [Eu(BTD)$_3$(DPBT)]@MnO_2 for tumor-targeting TGLI-MRI *in vivo*, the tumor xenograft models were established by implanting H22 cells (mouse hepatoma cell line) in the subcutaneous tissue of BALB/c nude mice (female) with a bodyweight of ~20 g. After the tumor size reached to 1.5~2 cm in diameter, six tumor-bearing BALB/c nude mice were randomly divided into two equal groups. For the experimental group, three mice were subcutaneously administered with 100 μL physiological saline solution containing the nanoprobe (11.5 μM Eu(BTD)$_3$(DPBT) mixed with 1.0 mM MnO_2 nanosheets) into the tumor and the opposite normal tissues. After that, the T_2-weighted MR images of the mice were taken at different time points (pre, 0.5, 1, 2, 3, 4, 5, 6 and 24 hour) following the injection. The MRI T_2 signal intensity analyses of the region of interest (ROI) were conducted using the Horos v3.3.1 software for Macintosh. To qualify the signal enhancement, the signal-to-noise ratio (SNR) was determined using the formula: $SNR = SI_{tumor}/SD_{noise}$, where SI and SD represent signal intensity and s.d, respectively. The other three tumor-bearing BALB/c nude mice in control group peritumorally injected with 100 μL physiological saline solution containing 2.0 mM NAC. After 0.5 h, a physiological saline solution of NEM (2.0 mM, 100 μL) was further peritumorally injected into the mice. After another 0.5 h, a physiological saline solution containing the nanoprobe was further peritumorally injected into the mice. Then the tumors were successively monitored by T_2-weighted MRI. In addition, the above described

mice were killed at 1 h post-injection of the nanoprobe, and the tumors were excised and stored at -20 ^{o}C for 24 h. The frozen tumor tissues were cryosectioned via microtome at -20 ^{o}C into slices of 30 μm thicknesses for the TGLI measurements on the microscope.

All of above animal studies were conducted in agreement with the guidelines of the Institutional Animal Care (No. 211003700000860) approved by the Animal Ethical and Welfare Committee (AEWC) of Dalian Medical University.

Statistical analysis

All the experiments were performed three times and the values were presented as the mean ± SD. Statistical comparison between the two groups was determined by Student's test. All statistical analyses were conducted with Excel (*$P < 0.05$, **$P < 0.01$, ***$P < 0.001$). A value of $P < 0.05$ was considered statistically significant.

2. Characterization of [Eu(BTD)$_3$(DPBT)]

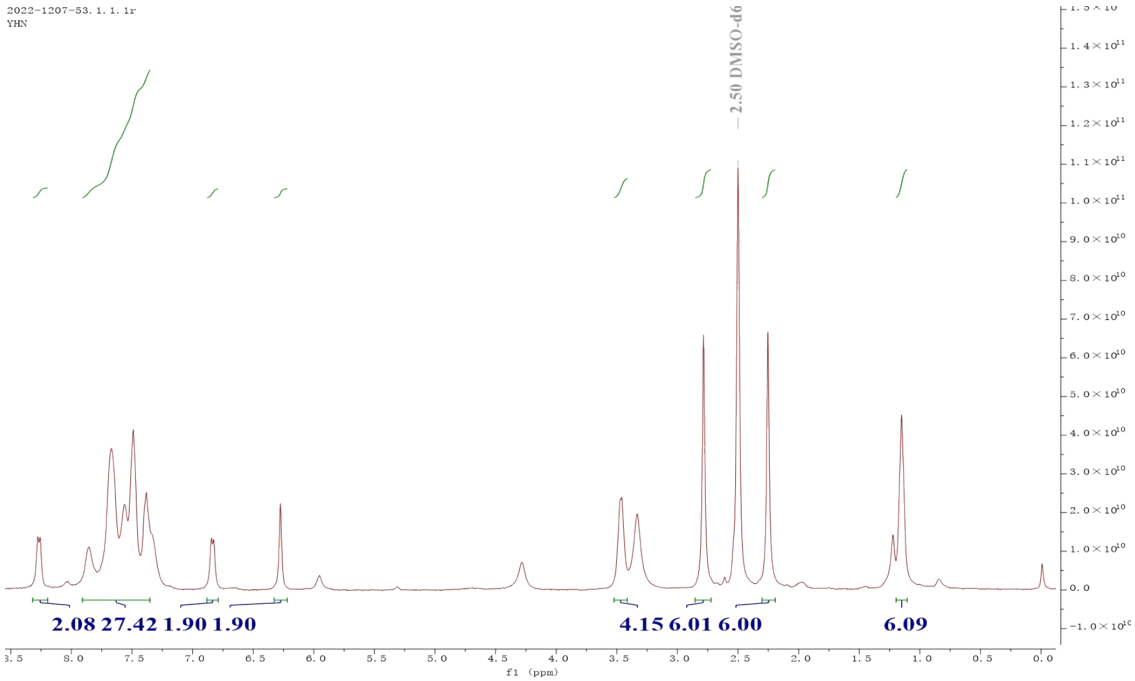

Fig. S1 ^{1}H NMR spectrum of [Eu(BTD)$_3$(DPBT)] (400 MHz, DMSO-d$_6$).

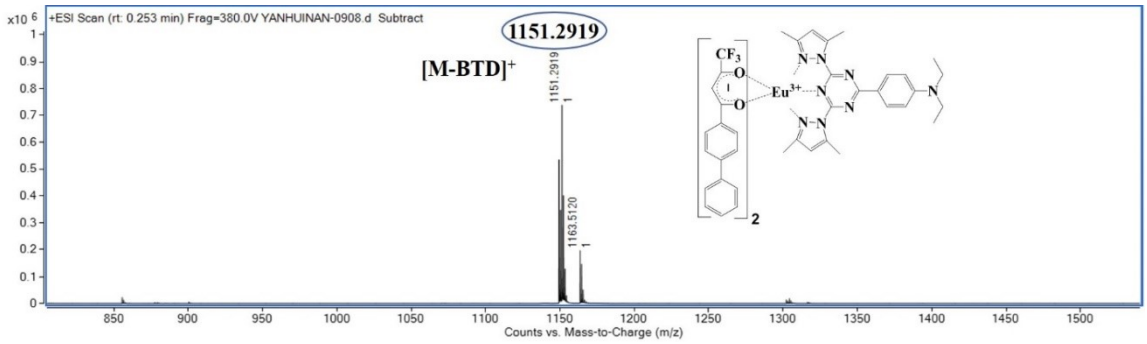

Fig. S2 ESI-HRMS spectrum of [Eu(BTD)$_3$(DPBT)].

3. Characterization of MnO_2 nanosheets

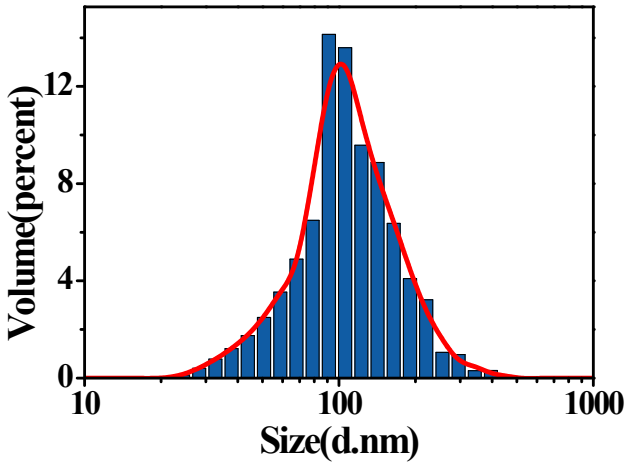

Fig. S3 Hydrated particle size distributions of MnO_2 nanosheets in 0.01M HEPES buffer (pH 7.4, containing 0.05% Triton X-100) determined by DLS.

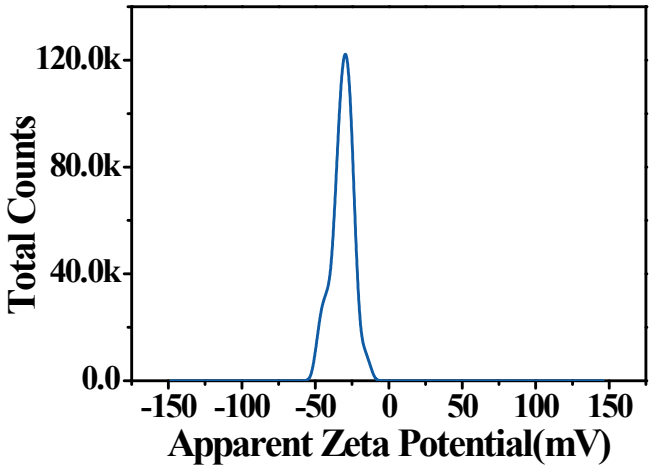

Fig. S4 Zeta potential distributions of MnO_2 nanosheets in 0.01M HEPES buffer (pH 7.4, containing 0.05% Triton X-100).

4. Luminescence properties of [Eu(BTD)$_3$(DPBT)]

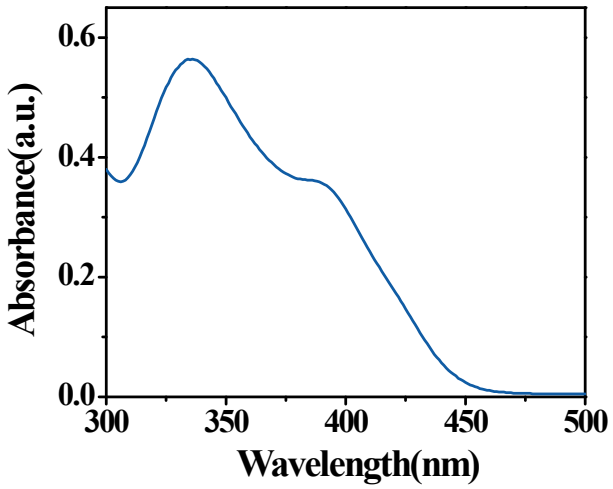

Fig. S5 UV-vis absorption spectrum of [Eu(BTD)$_3$(DPBT)] (8.0 μM) in 0.01 M HEPES buffer (pH 7.4, containing 0.05% Triton X-100).

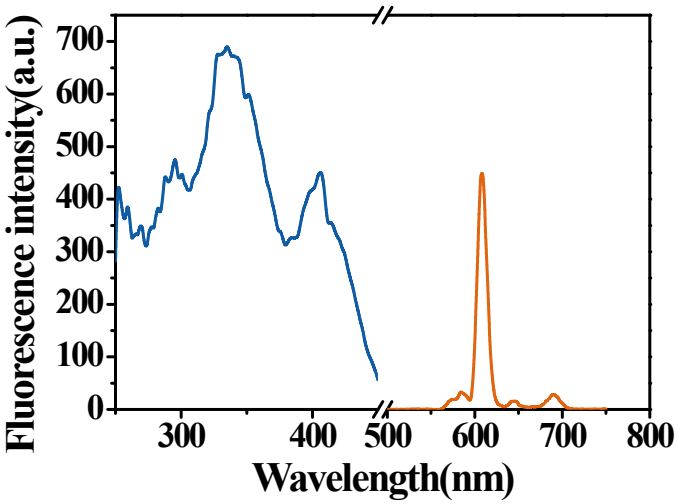

Fig. S6 Time-gated excitation (λ_{em} = 608 nm) and emission (λ_{ex} = 406 nm) spectra of [Eu(BTD)$_3$(DPBT)] (1.0 μM) in 0.01 M HEPES buffer (pH 7.4, containing 0.05% Triton X-100).

5. Bimodal TGL-MR responses of the nanoprobe [Eu(BTD)$_3$(DPBT)]@MnO_2 to GSH and H_2O_2

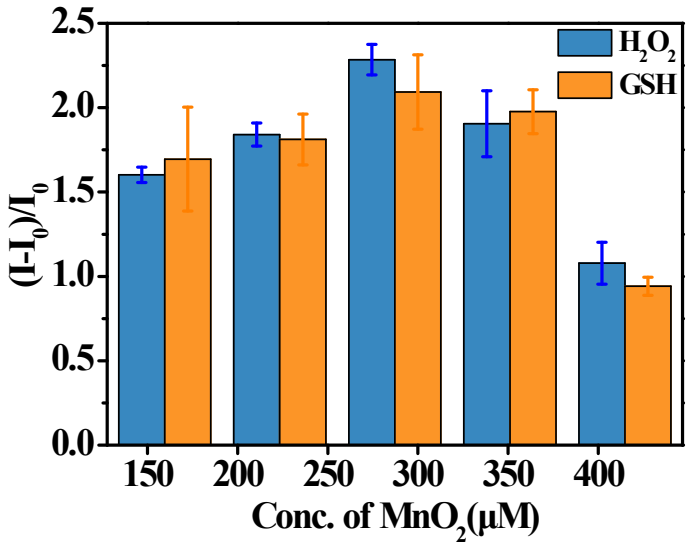

Fig. S7 TGL responses of the mixed solutions of 3.33 μM [Eu(BTD)$_3$(DPBT)] with different concentrations of MnO_2 nanosheets towards 6.67 μM GSH or H_2O_2 (I_0: TGL intensity of [Eu(BTD)$_3$(DPBT)]@MnO_2 in the absence of GSH or H_2O_2; I: TGL intensity of [Eu(BTD)$_3$(DPBT)]@MnO_2 reacted with GSH or H_2O_2.

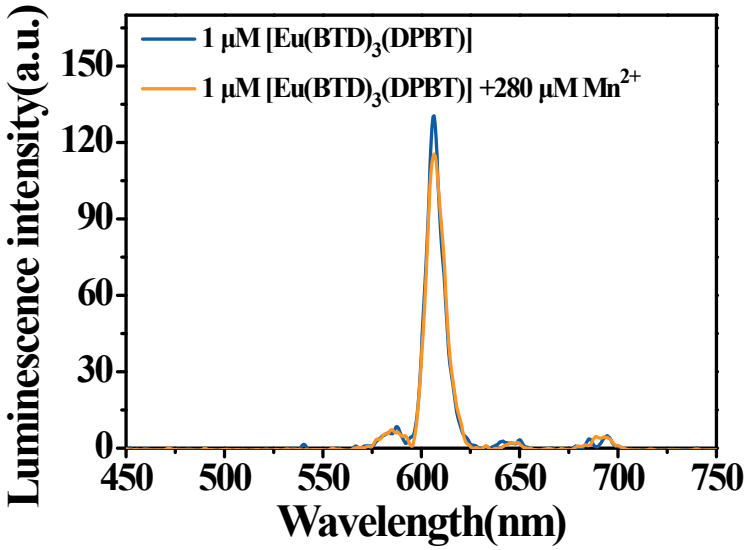

Fig. S8 Time-gated emission spectra (λ_{ex} = 406 nm) of [Eu(BTD)$_3$(DPBT)] (1.0 μM) in the absence and presence of Mn^{2+} ions (280 μM) in 0.01 M HEPES buffer (pH 7.4, containing 0.05% Triton X-100).

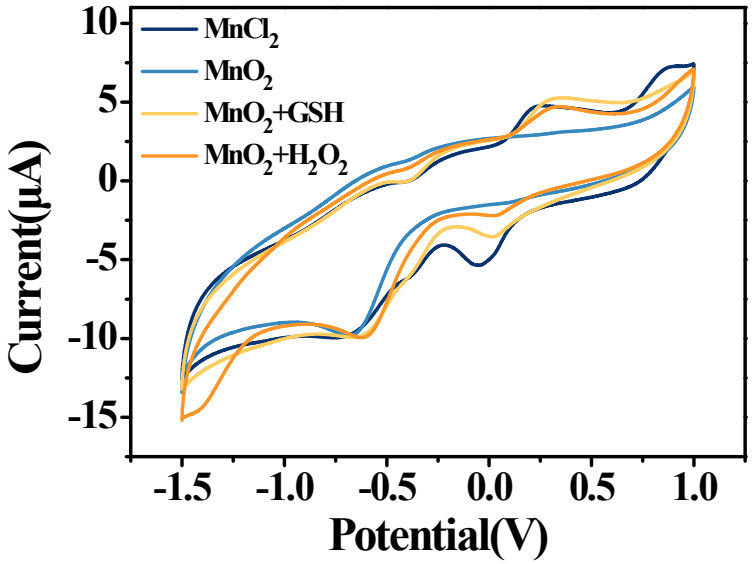

Fig. S9 CV profiles of Mn^{2+} ions and MnO_2 nanosheets in the absence and presence of GSH and H_2O_2.

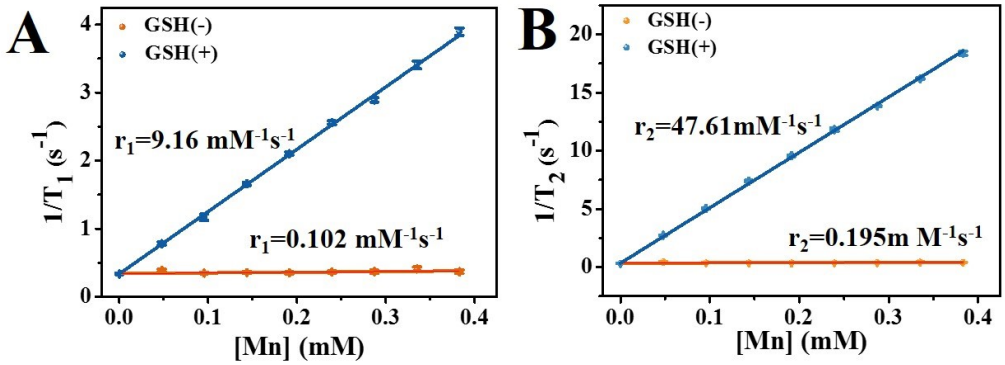

Fig. S10 Longitudinal (A) and transverse (B) relaxation rates of the nanoprobe $[Eu(BTD)_3(DPBT)]@MnO_2$ in the absence and presence of GSH.

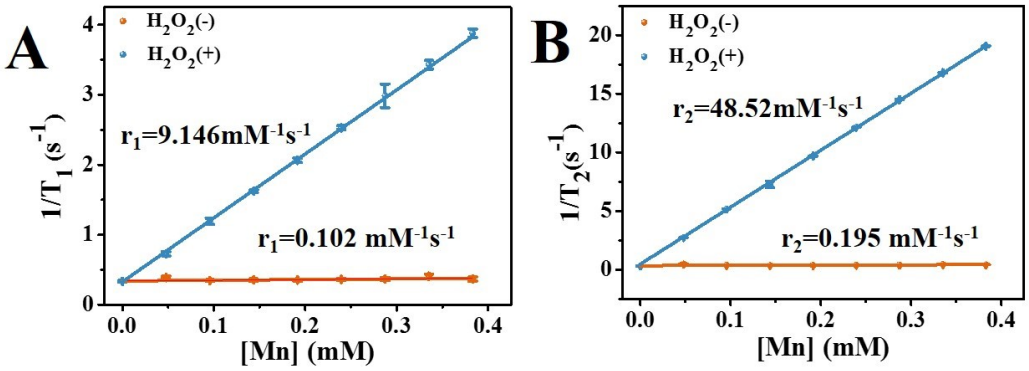

Fig. S11 Longitudinal (A) and transverse (B) relaxation rates of the nanoprobe [Eu(BTD)$_3$(DPBT)]@MnO_2 in the absence and presence of H_2O_2.

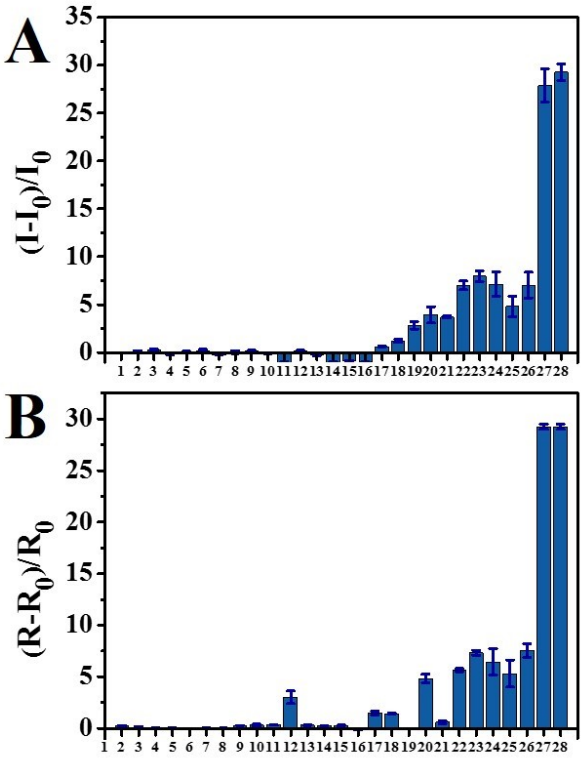

Fig. S12 TGL (A) and MR (B) responses of the nanoprobe [Eu(BTD)$_3$(DPBT)]@MnO_2 towards GSH (0.5 mM), H_2O_2 (0.5 mM) and other interferents (0.5 mM for Cys, Hcy, uric acid and Vc, 1.0 mM for other interferents). I_0: TGL intensity of the nanoprobe; I: TGL intensity of the nanoprobe reacted with various species. R_0: transverse relaxation rate of the nanoprobe; R: transverse relaxation of the nanoprobe reacted with various species. Species: 1: control; 2: Glu; 3: Val; 4: Pro; 5: Ala 6: His; 7: Thr; 8: Ser; 9: Asp; 10: Asp; 11: Cu^{2+}; 12: Gly; 13: HClO; 14: $^1O_2$; 15: ·OH; 16: NEM; 17: Na^+; 18: Trp; 19: NAC; 20: Tyr; 21: Zn^{2+}; 22: NADH; 23: Cys; 24:Hcy; 25: uric acid; 26:Vc; 27: GSH; 28: H_2O_2.

6. Cytotoxicity and biocompatibility investigations of the nanoprobe $[Eu(BTD)_3(DPBT)]@MnO_2$

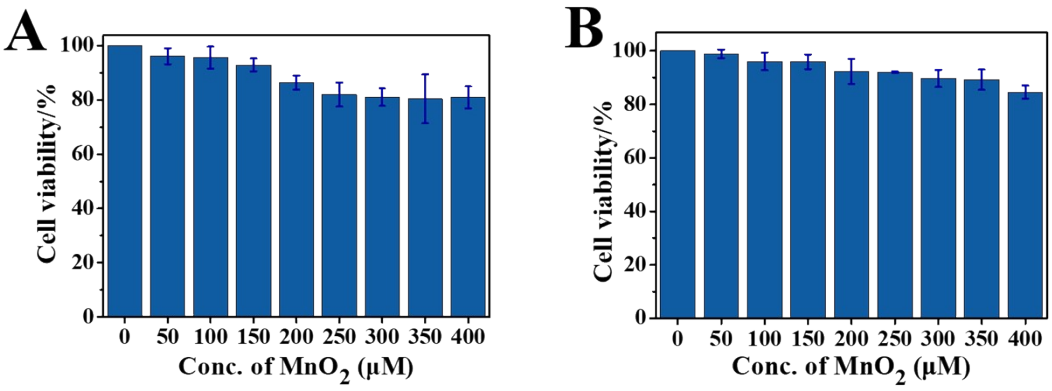

Fig. S13 Viabilities of HeLa (A) and LO2 (B) cells incubated with different concentrations of the nanoprobe $[Eu(BTD)_3(DPBT)]@MnO_2$ for 24 h.

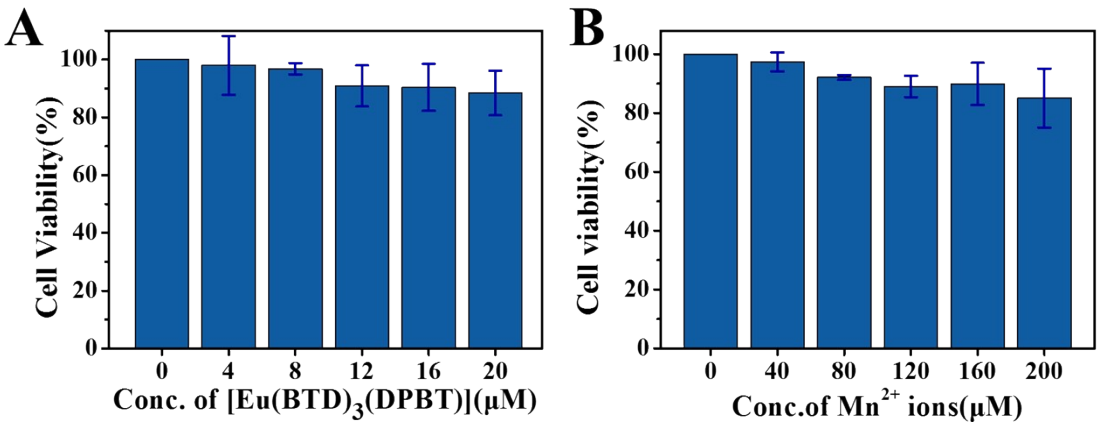

Fig. S14 Viabilities of HeLa cells incubated with different concentrations of $[Eu(BTD)_3(DPBT)]$ (A) and Mn^{2+} ions (B) for 24 h.

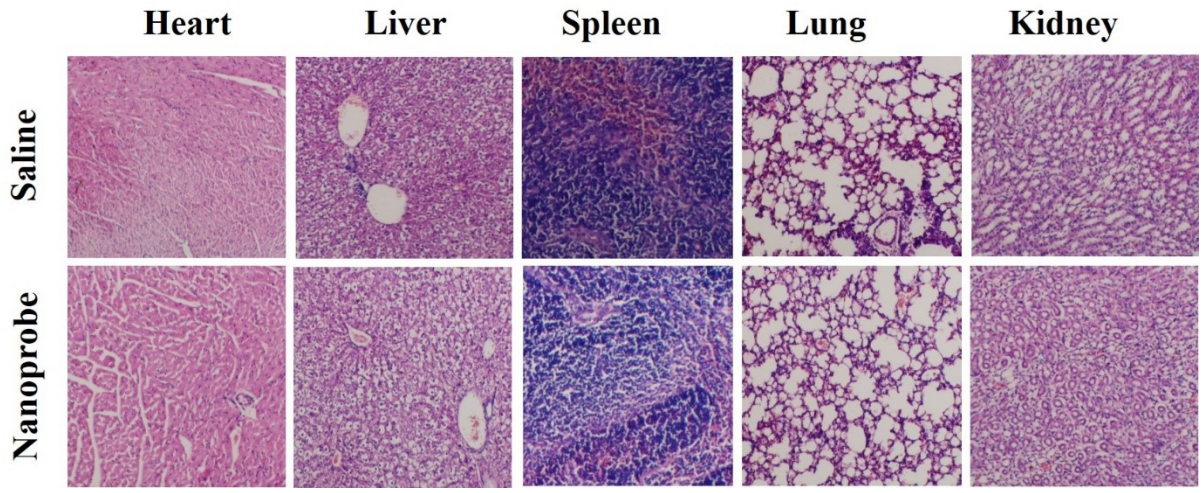

Fig. S15 Images of H&E stained main organs of the KM mice intravenously injected with physiological saline and the nanoprobe $[Eu(BTD)_3(DPBT)]@MnO_2$ for 24 h.

7. Cancer cell-targeted TGLI via the nanoprobe $[Eu(BTD)_3(DPBT)]@MnO_2$

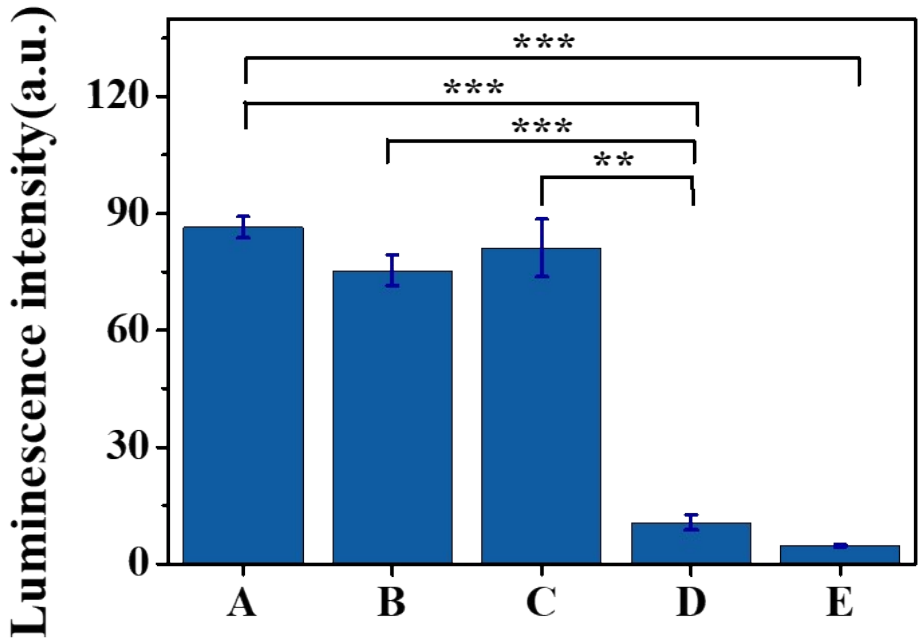

Fig. S16 Mean intracellular TGL intensities of different cells in TGL images of Figure 5. A: HeLa cells, B: HepG2 cells, C: MCF-7 cells, D: LO2 cells, E: NEM&NAC-pretreated HeLa cells (*$P < 0.05$, **$P < 0.01$, ***$P < 0.001$).

8. TGLI of the slices of tissue sections from tumor-bearing BALB/c mice

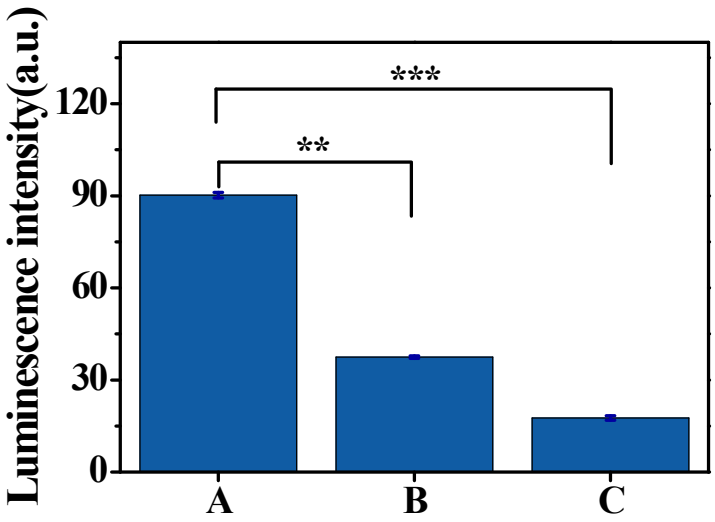

Fig. S17 Mean TGL intensities of the tissue sections in TGL images of Figure 7. A: tumor tissue slices, B: normal tissue slices, C: NAC&NEM-pretreated tumor slices (*$P < 0.05$, **$P < 0.01$, ***$P < 0.001$).

9. References

1. Y. Yuan, S. Wu, F. Shu and Z. Liu, *Chemical Communications*, 2014, **50**, 1095-1097.
2. J. Wu, G. Wang, D. Jin, J. Yuan, Y. Guan and J. Piper, *Chemical Communications*, 2008, DOI: 10.1039/B715054G, 365-367.
3. G. Wang, J. Yuan, K. Matsumoto and Z. Hu, *Analytical Biochemistry*, 2001, **299**, 169-172.
4. J. Shen, L.-D. Sun, J.-D. Zhu, L.-H. Wei, H.-F. Sun and C.-H. Yan, *Advanced Functional Materials*, 2010, **20**, 3707-3707.